

STUDY OF MIXING FREQUENCY PHASED ARRAY

Xiang Yong¹, Peng Chun², Peng Xuelian¹, Keren Shi³, Xu Xigang¹, Sun Wenlong¹

¹Time Group, Beijing, China, ²Peking University Health Science Center Beijing, China,

³NDT&E Lab., Dept. of Mechanical, Tsinghua University, Beijing, China

Abstract: A new method of ultrasound phased array — Mixing frequency Phased Array(MPA) in which elements excite respective frequency they may be not same each other and as well as normal phased array can focus and deflect is presented. In this paper, we discuss the theory of MPA based on interference principle, and simulate the distribution of MPA's sound field. Conclusionally, pressure intensity in focal area of MPA is enhanced observably, and range to be scanned which has effective contrast resolution is enlarged. This is specially useful for applications where HIFU therapy with more powerful energy and ultrasound imaging diagnostication with improvement of signal to noise ratio(SNR), attainability of beamforming and uniformity of imaging quality.

Introduction: Ultrasound phased arrays have been widely used for non-destructive testing in the past twenty years.[1-3] The beam can be found to control the deflexion and focus as shown in Fig.1 by controlling the phase of the excitation signal. Traditional phased arrays(PA) emit a single frequency

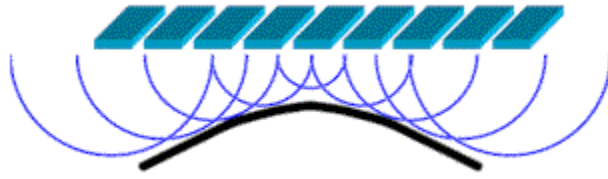


Fig.1 Phased Array

from all elements resulting in a fuzzy 2D image and insufficient power in the focus region.[4,5] Better systems have been developed using wide frequency band material and electronic control.

Results: This paper describes a new mixed frequency phased array(MPA) in which the frequencies of the various elements are independent and which provides improved arrays control. A theoretical model of the array based on the interference principle was used to analyze the MPA sound distribution.

Discussion:

The vibrating surface of transducers of all shapes and sizes can be modeled as many point sources. Therefore each small area of the ultrasound transducer can be modeled as a vibrating piston source set in a hard baffle plate. The sound pressure at any point (x, y, z) can then be calculated by:

$$p(x, y, z) = \frac{j\rho c}{\lambda} \int_s u \frac{e^{-(\alpha+jk)r}}{r} ds \quad (4)$$

Where the integration includes all the effective vibrating surfaces.

The corresponding sound intensity of the point would be:

$$I(x, y, z) = \frac{1}{2\rho c} p^2 \quad (5)$$

The sound pressure and sound intensity at any point in the field can then be calculated numerically. Eq.4 can be integrated using the Huygen criterion, but numerical quadra have to simplify. The fast algorithm given by Ocheltree and Frizzell[9] was used to numerically simulate the sound field from the elementary. The rectangular piston array was divided into a series of rectangular elements as shown in Fig.2.

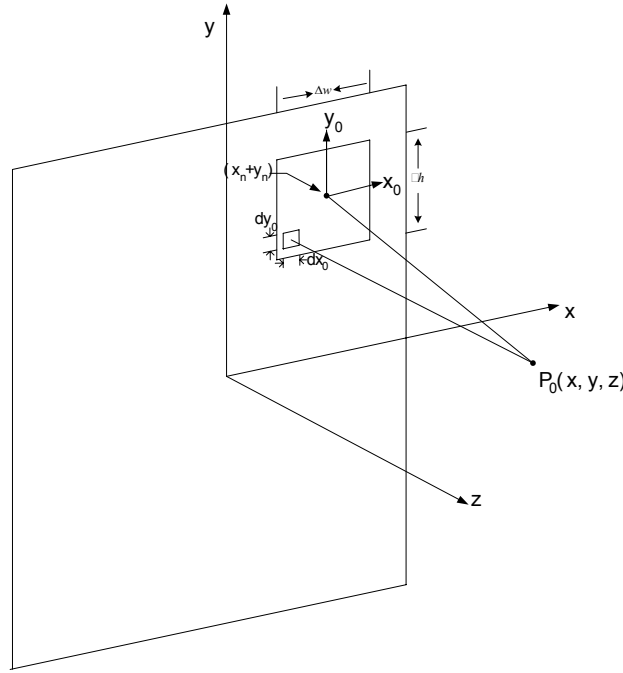


Fig.2 Coordinate system for numerical algorithm

These elements can be bigger than point sources, but small enough to allow accurate integration using:

$$p(x, y, z) = \frac{j\rho c \Delta A}{\lambda} \sum_{n=1}^N \frac{u_n}{R} e^{-(\alpha + jk)R} \sin c \frac{kx'_n \Delta w}{2R} \sin c \frac{ky'_n \Delta h}{2R} \quad (6)$$

Eq.6 assume that: $\frac{x_0^2}{2R} + \frac{y_0^2}{2R}$ is negligible 0, $r \approx R$, and $e^{\alpha x'_n x_0 / R} \approx 1$. Since the maximum absolute values of x_0 and y_0 are $\Delta w / 2$ and $\Delta h / 2$ respectively, these assumptions can be written as:

- (1) $\cos(k\Delta w^2 / 8R + k\Delta h^2 / 8R) \approx 1$
- (2) $r \approx R$
- (3) $e^{\alpha(x'_n \Delta w + y'_n \Delta h) / 2R} \approx 1$

These conditions on Δw and Δh limit the applicability of Eq. 6. Condition (1) can be transformed to $\pi \gg k\Delta w^2 / 8R$ or $R \gg \Delta w^2 / 4\lambda$. Since $z < R$, condition (1) can also be written as $z \gg \Delta w^2 / 4\lambda$. Using a proportionality constant C, the condition can be written as :

$$\Delta w \leq \sqrt{\frac{4\lambda z}{C}} \quad (7)$$

In this paper, C was assumed to be 10 and Eq.7 was use to determine Δw to divide the rectangular piston into rectangular elements that would satisfy the limits imposed by Eq.6. The

number of elements, N , must also satisfy a similar condition for Δh . The condition for Eq.7 for deciding Δw and Δh also satisfies conditions (2) and (3).

The algorithm for calculating the sound distribution from the rectangular pistons can be generalized as:

1. Select z (the position on the axis z) .
2. Calculate the values of Δw and Δh using Eq.7 and divide the rectangular piston into N rectangular elements with areas $\Delta A = \Delta h \Delta w$. All the points at a distance z are, therefore in the far field of the rectangular elements.
3. With calculate the sound pressure produced by all the rectangular elements using Eq.8.
4. Repeat 1 and 3 for a different z .

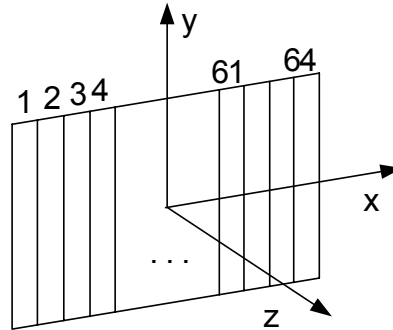


Fig.3 Linear Array

The simulated sound distribution of a focusing and deflecting sound field form a linear phased array with 64 elements is shown in Fig.3. During simulation we make Field II as a program reference.[10,11] Two schemes was used to study the changes in the sound field before and after mixing the frequency: the selection of any point on the focusing plane or the selection of the center frequency. The transducer array design used in the calculation had 64 elements in the x-y plane with the parameters listed in Table 1.

Table 1. The parameters in simulation

Intensity of the array element source	5 W/cm ²
Velocity of sound c	1540 m/s
Density ρ	1000 kg/m ³
Modulus of decay α	0.007 dB/mm
Element size	15 mm x 1 mm
Interval between elements	1.2 mm

Consider for example a focusing point $F(10,0,100)$ The conventional constant frequency phased method would require all the elements in the array to radiate ultrasound signals at the same frequency. The phased array would then produce a nonuniform sound distribution and so the sound intensity at the focal point F would also vary greatly. The sound intensity distributions on the x-y plane for are given in Fig.4a 1 MHz, Fig.4b 2 MHz and Fig.4c 3 MHz frequencies. Fig.4d shows the relation between the sound intensity at point F and the ultrasound. frequency Fig.4d shows that far point F , the sound intensity is greatest at the frequency of 2 MHz.

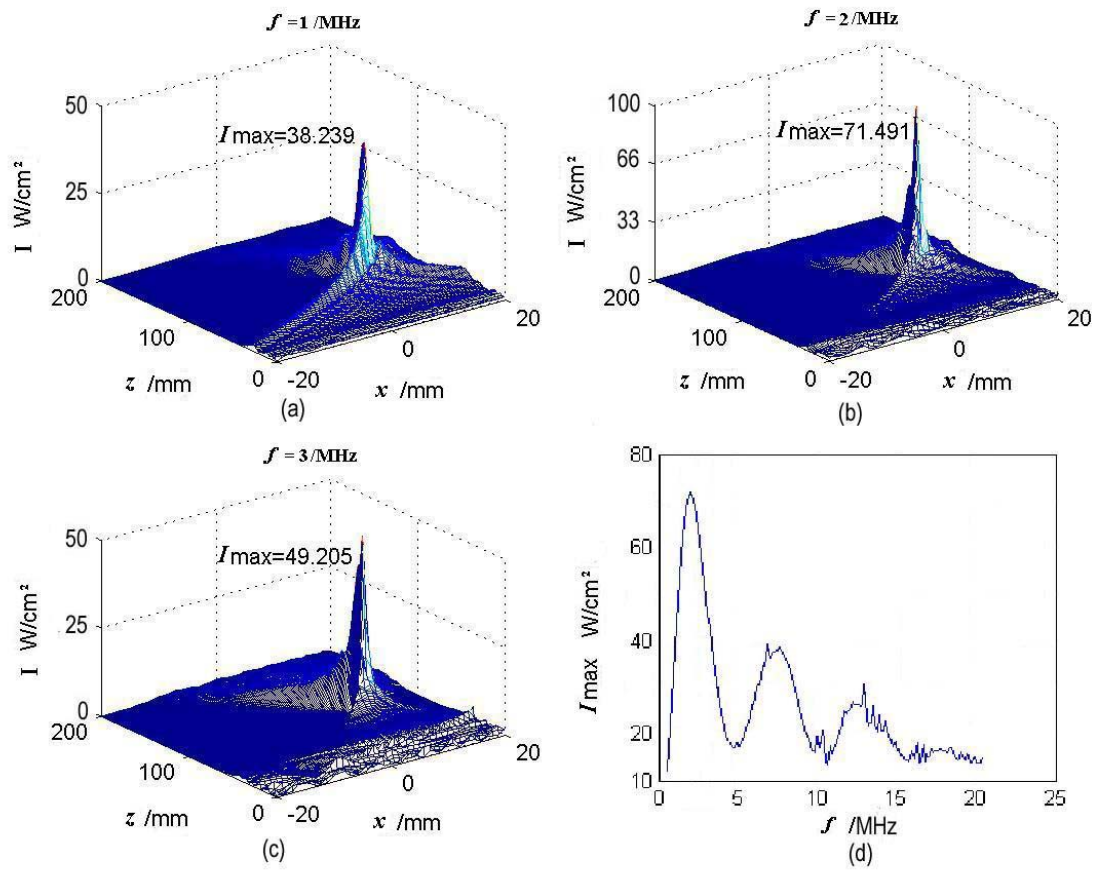


Fig.4. Phased array sound field

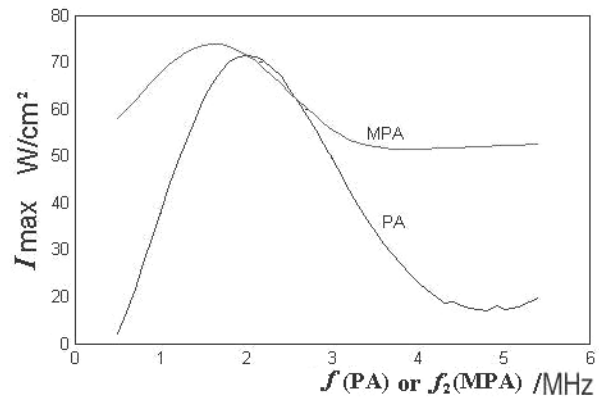


Fig.5 PA and MPA of F(10,0,100)

Therefore to design a mixed frequency phased array using for the array in Fig.5 with 64 elements, the 48 elements in the middle of the array would be given the center frequency of $f_1 = 2$ MHz, while the 8 elements on both sides would have frequencies f_2 varying from 0.5 MHz to 20 MHz. Fig.5 shows the relation between the sound intensity at point F and the sound frequency of the elements on both sides of the mixing phased array. For the constant frequency phased array while $f = 2$ MHz, $Max = 71.5 \text{ W/cm}^2$, but for the mixed frequency phased array. $Max = 73.9 \text{ W/cm}^2$ for $f_2 = 1.6$ MHz. Therefore the mixed frequency phased array can increase the sound intensity and the acoustic energy density in the focal area compared to a conventional constant frequency phased array. Reducing the frequency of the elements far from the array focus increases the maximum sound intensity in the focal area.

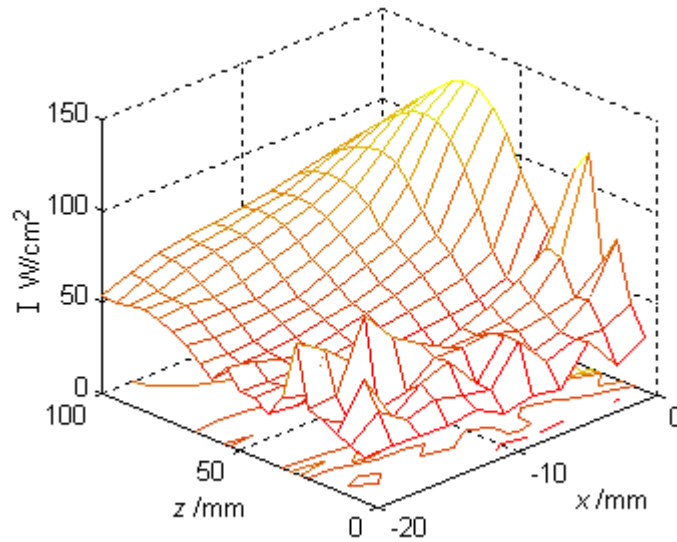
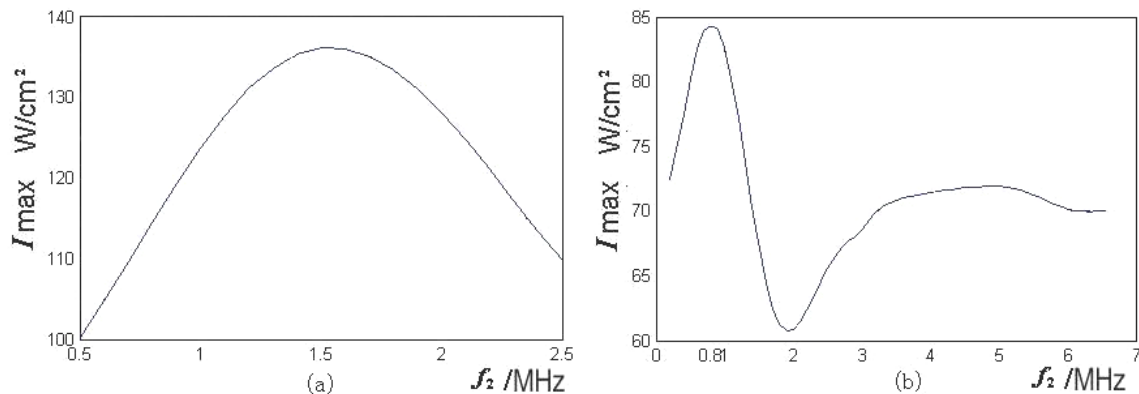


Fig.6 Sound intensity distribution

A center frequency of 2 MHz was used to further study. First, the maximum sound intensity on the focal plane with the constant frequency phased array can be seen in Fig.6 to occur at point F1(0,0,70) with a Maximum intensity of 128.1 W/cm^2 for a constant frequency of 2 MHz. With the Mixed frequency array with the 2 MHz center frequency, the sound intensity at F1(0,0,70) shown in Fig.9a. for $f_2 = 1.5$ MHz, $Max = 136.1 \text{ W/cm}^2$.

At another point F2(-8,0,70) off the focus, as shown in Fig.7b, for a constant frequency phased array with $f = 2$ MHz, $Max = 60.9 \text{ W/cm}^2$, with the mixed frequency array, $Max = 84.4 \text{ W/cm}^2$ with $f_2 = 0.8$ MHz.

Fig.7 Sound field at F1(0,0,70) and F2(-8,0,70) for the MPA



The result in Fig.7 also show that the sound intensity in the focal area is increased and the acoustic energy is enhanced with the mixed frequency phased array, compared with a single frequency phased array. Proper reduction of the ultrasound frequency of elements far from the array focus increases the sound intensity in the focal area. In addition, the sound intensity away from the focus center of plane was increased more obviously before and after mixing frequency.

The -3 dB and -6 dB scan range are compared in Fig.8 for the mixed frequency phased array using 2 MHz in the center and 1.5 MHz on the side (Fig.8a), a 2 MHz constant frequency array (Fig.8b), and a 1.5 MHz constant frequency phased array (Fig.8c). The mixed frequency phased array had a larger scanning area which would improve the usefulness of the phased sound array.

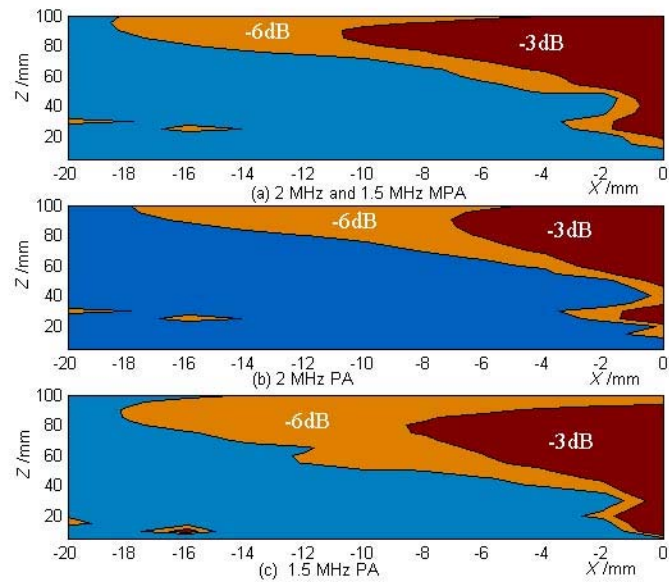


Fig.8 Sound intensity distribution

Conclusions: For ultrasound phased array systems, the contrast resolution is closely related to the energy density and the maximum intensity of the focus in the field. Increased sound intensities give better signal-to-noise ratios, and higher image contrast. A mixed frequency phased array was analyzed theoretically using superposition of the sound waves and the directivity of the ultrasound array. The simulation of the mixed frequency phased array sound field showed that the mixed frequency phased array with optimum frequency parameters can increase the energy density in the focal area to provide higher signal-to-noise ratios. The scanning area of the phased array is also expanded, which improves usefulness availability of the sound beam.

References:

- [1] Calmon, P, Mahaut, S, Chatillon, S, Roy, O. Simulation of phased array techniques for realistic NDE configurations. In: Ultrasonics Symposium, 2002. IEEE ,Volume: 1, Pages:723 - 727
- [2] Li J, Rose J.L. Implementing guided wave mode control by use of a phased transducer array. In: Ultrasonics, Ferroelectrics and Frequency Control, 2001: Volume: 48 , Pages:761 – 768
- [3] Kouki Nagamune, Yutaka hata. Automated extraction of buried pipes from 3D ultrasonic images by fuzzy inference. In: Proceedings of ICSP2000: Volume: 2 , Pages:877 - 881
- [4] A.McNab, D.Reilly, A.Potts, M.Toft. Role of 3D graphics in NDT data processing. In: Measurement and Technology, IEE Proceeding 2001: Volume: 148 , Pages:149 - 158
- [5] Saeid Sanei, Tracey K.M .Lee. An Architecture for High Speed Ultrasound Image Capture and Real-time 3D Reconstruction. In: Electronic Design, Test and Applications (DELTA '02), 2002. Proceedings. Pages:326 - 330
- [6] Doehle A, Hoffelner J, Landes H, Lerch R. Numerical simulation of high-intensity standing wave fields. In: Ultrasonics Symposium, 2002: Volume: 1 ,Pages:543 - 546
- [7] Lewin P A, Schafer M E. Wide-band piezoelectric polymer acoustic sources. In: Ultrasonics, Ferroelectrics and Frequency Control, 1988. Volume: 35 , Issue: 2 , March 1988 Pages:175 - 185
- [8] Xiang Yong, Huo Jian, Shi Keren, Chen Yifang. Study of characteristics of sound field in mixing phased array. Key Engineering Materials, 2004

- [9] Kenneth B. Ocheltree, Leon A. Frizzell. Sound Field Calculation for Rectangular Sources. In: IEEE Transaction on Ultrasonics, Ferroelectrics, and Frequency Control. 1989: Vol36 (2) . 2-4
- [10] Jensen J A, Nikolov I. Fast simulation of ultrasound images. In: Ultrasonics Symposium, 2000: Volume: 2 ,Pages:1721 - 1724
- [11] Jensen J A, Svendsen N B. Calculation of pressure fields from arbitrarily shaped, apodized, and excited ultrasound transducers. In: Ultrasonics, Ferroelectrics and Frequency Control, 1992: Volume: 39, Pages:262 – 267